Cell. Mol. Life Sci. (2014) 71:899–916
DOI 10.1007/s00018-013-1406-1

Cellular and Molecular Life Sciences

RESEARCH ARTICLE

Double deficiency of cathepsins B and L results in massive secretome alterations and suggests a degradative cathepsin-MMP axis

Stefan Tholen · Martin L. Biniossek · Martina Gansz · Theresa D. Ahrens · Manuel Schlimpert · Jayachandran N. Kizhakkedathu · Thomas Reinheckel · Oliver Schilling

Received: 28 March 2013 / Revised: 6 June 2013 / Accepted: 10 June 2013 / Published online: 29 June 2013

Abstract Endolysosomal cysteine cathepsins functionally cooperate. Cathepsin B (Ctsb) and L (Ctsl) double-knockout mice die 4 weeks after birth accompanied by (autophago-) lysosomal accumulations within neurons. Such accumulations are also observed in mouse embryonic fibroblasts (MEFs) deficient for Ctsb and Ctsl. Previous studies showed a strong impact of Ctsl on the MEF secretome. Here we show that Ctsb alone has only a mild influence on extracellular proteome composition. Protease cleavage sites dependent on Ctsb were identified by terminal amine isotopic labeling of substrates (TAILS), revealing a prominent yet mostly indirect impact on the extracellular proteolytic cleavages. To investigate the cooperation of Ctsb and Ctsl, we performed a quantitative secretome comparison of wild-type MEFs and *Ctsb*$^{-/-}$ *Ctsl*$^{-/-}$ MEFs. Deletion of both cathepsins led to drastic alterations in secretome composition, highlighting cooperative functionality. While many protein levels were decreased, immunodetection corroborated increased levels of matrix metalloproteinase (MMP)-2. Re-expression of Ctsl rescues MMP-2 abundance. Ctsl and to a much lesser extent Ctsb are able to degrade MMP-2 at acidic and neutral pH. Addition of active MMP-2 to the MEF secretome degrades proteins whose levels were also decreased by Ctsb and Ctsl double deficiency. These results suggest a degradative Ctsl—MMP-2 axis, resulting in increased MMP-2 levels upon cathepsin deficiency with subsequent degradation of secreted proteins such as collagen α-1 (I).

Keywords Cathepsin L · Cathepsin B · MMP-2 · Proteomics · TAILS · Proteolysis

Abbreviations

ADAMTS	A disintegrin and metalloproteinase with thrombospondin motifs
BM	Basement membrane
BSA	Bovine serum albumin
CCM	Cell-conditioned media
Ctsb	Cathepsin B
Ctsd	Cathepsin D
Ctsl	Cathepsin L
Ctsz	Cathepsin Z
DMEM	Dulbecco's modified Eagle's medium
DTT	Dithiothreitol
E64d	(2S, 3S)-*trans*-epoxysuccinyl-L-leucylamido-3-methylbutane ethyl ester

Electronic supplementary material The online version of this article (doi:10.1007/s00018-013-1406-1) contains supplementary material, which is available to authorized users.

S. Tholen · M. L. Biniossek · M. Gansz · T. D. Ahrens · M. Schlimpert · T. Reinheckel · O. Schilling (✉)
Institute for Molecular Medicine and Cell Research, University of Freiburg, Stefan Meier Strasse 17, 79104 Freiburg, Germany
e-mail: oliver.schilling@mol-med.uni-freiburg.de

S. Tholen · M. Gansz · T. D. Ahrens
Faculty of Biology, University of Freiburg, 79104 Freiburg, Germany

J. N. Kizhakkedathu
Centre for Blood Research, University of British Columbia, Vancouver, BC V6T 1Z3, Canada

J. N. Kizhakkedathu
Department of Pathology and Laboratory Medicine, University of British Columbia, Vancouver, BC V6T 1Z3, Canada

J. N. Kizhakkedathu
Department of Chemistry, University of British Columbia, Vancouver, BC V6T 1Z3, Canada

T. Reinheckel · O. Schilling
BIOSS Centre for Biological Signaling Studies, University of Freiburg, 79104 Freiburg, Germany

ECM	Extracellular matrix
EDTA	Ethylene diamine tetraacetic acid
FACS	Fluorescence-assisted cell sorting
Fc	Fold change
GFP	Green fluorescent protein
GO	Gene ontology
HPLC	High-performance liquid chromatography
IGF	Insulin-like growth factor
IGFBP	Insulin-like growth factor-binding protein
IRES	Internal ribosomal entry site
Lamp	Lysosome-associated membrane glycoprotein
LC–MS/MS	Liquid chromatography tandem mass spectrometry
LDH	Lactate dehydrogenase
LEF	Lymphocyte enhancer factor
MEF	Mouse embryonic fibroblast
MMP	Matrix metalloprotease
MS	Mass spectrometry
NCAM	Neural cell adhesion molecule
ON	Overnight
PBS	Phosphate-buffered saline
PICS	Proteomic identification of protease cleavage sites
PMSF	Phenylmethanesulfonyl fluoride
POSTN	Periostin
PVDF	Polyvinylidene fluoride
SCX	Strong cation exchange
SDS	Sodium dodecylsulfate
STRING	Search tool for the retrieval of interacting genes
SFRP	Secreted frizzled-related protein
TAILS	Terminal amine isotopic labeling of substrates
TCF	T-cell factor
wt	Wild-type
XIC	Extracted ions chromatograms

Introduction

Cathepsins belong to the C1-family of papain-like cysteine proteases with 11 members in man [1] and 18 members in mouse [2]. Cysteine cathepsins are predominantly described as endopeptidases such as cathepsin L, while cathepsin B shows additional carboxydipeptidase activity [3]. Localized in the endosomal/lysosomal compartment, cathepsins were traditionally thought to participate in lysosomal protein turnover. Meanwhile, cathepsins have been described in additional locations such as the extracellular space [4–6] (for review, [7, 8] and linked to more specific functions in many physiological and pathological processes in which they act as digestive as well as regulatory proteases [9].

The ubiquitously expressed cathepsins B (Ctsb) and L (Ctsl) are upregulated, translocated to the cell surface, and secreted during pathological processes such as tumor progression [10, 11]. The complex set of proteins secreted by living cells is defined as the secretome [12]. A previous secretome analysis of Ctsl-deficient MEFs demonstrated an impact of Ctsl on secretome composition, especially affecting abundances of extracellular matrix (ECM) components, signaling proteins, and further proteases as well as endogenous protease inhibitors [13]. Strong alterations in ECM composition and extracellular proteolysis have been observed in vivo in a proteomic analysis of Ctsl-deficient skin and to a lesser extent in Ctsb-deficient skin. Among others, Ctsl deficiency altered protein abundance of cathepsin D, cystatin B and M/E, periostin as well as collagens [14]. Mice deficient in Ctsb and Ctsl die 4 weeks after birth caused by neuronal cell death in the cerebral cortex and a degeneration of cerebellar Purkinje and granule cells [15, 16]. Since neurons of single-gene-deficient mice develop normally, mutual compensation between Ctsb and Ctsl in vivo has been suggested [15, 17].

To elucidate if cooperative functionality of Ctsb and Ctsl affects extracellular biology, we performed a proteomic analysis of Ctsb single-deficient and $Ctsb^{-/-}$ $Ctsl^{-/-}$ MEFs. To determine how Ctsb alone contributes to secretome composition, we compared Ctsb knockout mouse embryonic fibroblasts (MEFs) to wild-type MEFs using a twofold strategy. This consists first of a gel-free quantitative proteomic approach to investigate alterations in protein abundance [18, 19]. Second, terminal amine isotopic labeling of substrates (TAILS) [20] was performed to identify Ctsb-dependent cleavage sites and to determine alterations in the secretome cleavage pattern. This strategy has already been successfully applied to the proteomic analysis of Ctsl-deficient MEFs and wild-type MEFs [13]. To establish whether alterations in secretome composition potentiate upon double deletion of Ctsb and Ctsl, a quantitative proteome comparison was performed comparing Ctsb and Ctsl double-knockout MEFs to wild-type MEFs. All approaches were performed in true biological replicates with each MEF cell line originating from a different mouse, which minimizes bias caused by individual biological variability, which typically exceeds technical variability [21]. Selected proteomic data were corroborated by immunodetection.

Whereas single Ctsb depletion has a limited effect on secretome composition, drastic alterations in secretome composition are observed upon depletion of Ctsb and Ctsl, pointing to a strong synergistic functionality of both proteases. TAILS revealed Ctsb-dependent cleavage sites upon Ctsb depletion in both biological replicates. Moreover, we demonstrate that Ctsl and to a lesser extent Ctsb are involved in MMP-2 degradation and processing, resulting in increased MMP-2 levels upon Ctsb and Ctsl depletion.

While MMP–2 accumulates, almost all other significantly affected proteins upon Ctsb and Ctsl deficiency, like collagen α-1 (I), display a decreased abundance.

Materials and methods

Generation and culturing of cell lines

Mouse embryonic fibroblasts were prepared as described previously [22]. Two cell lines were generated from wild-type FVB mice, two cell lines were generated from *Ctsb*$^{-/-}$ FVB mice, and two cell lines were generated from *Ctsb*$^{-/-}$ *Ctsl*$^{-/-}$ FVB mice. Ctsl was re-expressed in Ctsl-deficient and wild-type MEFs, as described previously [14]. Cells were cultured in Dulbecco's modified Eagle's medium (DMEM, PAN, Aidenbach, Germany) supplemented with 10 % fetal calf serum (PAN) and 1 % penicillin/streptomycin stock solution (Gibco/Invitrogen, Paisley, UK) at 37 °C in humidified air containing 5 % CO_2. All cell lines were immortalized with the simian virus-40 large-T antigen (pBABE-puro SV40 LT; Addgene, Cambridge, MA, USA) [23] with a retroviral transfection procedure [24].

To analyze the protein abundance of MMP-2 upon different growth conditions, MEFs were grown on coated plates coated with either fibronectin (BD Biosciences, Bedford, MA, USA) or collagen type IV (BD Biosciences). MEFs were cultured in serum-free DMEM, serum-free DMEM without arginine and lysine (Silantes, Munich, Germany) or serum-free DMEM containing 0.1 % albumin without arginine and lysine.

Proliferation and cell viability

Proliferation was measured using the xCELLigence system (Roche, Mannheim, Germany); 15,000 cells were grown per well in tissue culture plates, called E plates (Roche, Mannheim, Germany). Cell growth was monitored in real time by measuring electrical impedance across interdigitated gold micro-electrodes integrated in the bottom of Roche E-plates.

To measure cell viability, 100,000 cells per well were seeded in 3.8 cm^2 wells. After adherence, cells were washed three times with pre-warmed phosphate-buffered saline (PBS) and switched to serum-free DMEM without phenol red for 24 h. Cell viability was assayed by LDH activity according to the manufacturer's instructions (CytoTox 96 non-radioactive cytotoxicity assay, Promega, Madison, WI, USA).

Cell stainings

Acridine orange staining was performed by seeding 50,000 cells per well on cover slips in 24-well plates. After 24 h, cells were incubated with acridine orange (Invitrogen, Eugene, OR, USA) at a dilution of 1:25,000 in culture medium from a 10 mg/ml stock for 15 min at 37 °C in humidified air containing 5 % CO_2. Slides were washed with PBS and analyzed using the Axio fluorescence microcope (Zeiss) with excitation channels Texas Red (596/615 nm).

Lamp-1 staining was performed by seeding 45,000 cells per well on cover slips in 24-well plates. After overnight incubation, cells were fixed with 4 % PFA in PBS for 15 min at room temperature, washed with PBS and permeabilized with 0.2 % Triton X-100 in PBS for 7 min at room temperature. Afterwards cells were treated for 4 min with −20 °C cold acetone, washed with PBS, and blocked with 5 % BSA for 30 min. Lamp-1 antibody (1:700; catalog no. ab25245; Abcam, Cambridge, UK) was applied in 5 % BSA over night at 4 °C. After washing with PBS secondary antibody (Alexa 488 goat anti-rat, 1:1,000: Invitrogen, A11006) was applied in 5 % BSA for 1 h at room temperature. Cells were washed with PBS and nuclei stained for 5 min with 2 µg/ml Hoechst (Fluka/Sigma, Munich, Germany). After a final wash with PBS, cover slips were mounted with Permafluor (Labvision, Fremont, CA, USA) and analyzed using the Axio fluorescence microcope (Zeiss).

Quantitative secretome comparison

Cells were grown to near confluence in serum-containing medium, washed three times with pre-warmed PBS, and switched to serum-free DMEM without phenol red. Cell-conditioned media were collected after 24 h, supplemented with protease inhibitors (5 mM EDTA, 0.01 mM E64, 1 mM PMSF), centrifuged, and filtered using a 0.2-µm filter to ensure removal of dead cells. Protein content was measured using the Bradford assay (BIO-RAD, Munich, Germany); 300 µg of protein was used per condition for the quantitative secretome comparison.

Preparation of mass spectrometry samples was performed as described previously, including stable isotope labeling with either d_2^{13}C-formaldehyde ("heavy," employed for wild-type skin samples) or d_0^{12}C formaldehyde ("light," employed for cathepsin-deficient skin samples) for quantitative comparison and pre-fractionation by strong cation exchange (SCX) chromatography [13]. Labeling was performed after tryptic digestion. LC–MS/MS analysis is described in the corresponding section. Data were converted to mzXML format [25] using Proteowizard [26] with centroiding of MS1 and MS2 data. Peptide sequences were identified by X! Tandem (version 2010.12.01) [27], including cyclic permutation, in conjunction with PeptideProphet (part of version 4.3.1 of the Trans Proteomic Pipeline) [28] and a decoy search strategy: the complete mouse

proteome file was downloaded from UniProt [29] on 16 October 2011, comprising 44,819 protein sequences. It was appended with an equal number of randomized sequences, derived from the original mouse proteome entries. The decoy database was generated with DBToolkit [30]. Tryptic cleavage specificity with no missed cleavage sites was applied. Mass tolerance was 10 ppm for parent ions and 0.3 Da for fragment ions. Static modifications are cysteine carboxyamidomethylation (+57.02 Da), lysine and N-terminal dimethylation (light formaldehyde 28.03 Da; heavy formaldehyde 34.06 Da). X!Tandem results were further validated by PeptideProphet at a confidence level of >95 %. Corresponding protein identifications are based on the ProteinProphet algorithm with a protein false discovery rate of <1.0 %. The relative quantitation for each protein was calculated from the relative areas of the extracted ion chromatograms of the precursor ions and their isotopically distinct equivalents using the ASAPratio [31] algorithm. In our experience (shared by others, [32]), ASAPratio occasionally displays inaccuracies with regard to background removal and separation of neighboring peaks along a given mass trace. To prevent inaccurate protein quantization, protein ratios were also analyzed by the XPRESS [33] algorithm. Proteins were considered if XPRESS and ASAPratio yielded convergent results. Reported Fc values are based on normalized ASAPratio.

Cleavage site analysis with TAILS

Terminal amine isotopic labeling of substrate was performed using formaldehyde labeling according to the original publications [20, 34]; 2 mg of protein was used per condition. After tryptic digest samples were desalted using a reversed phase C18 column, prefractionated by SCX as described, and desalted using self-packed C18 STAGE tips (Empore, USA) [35]. LC–MS/MS analysis is described in the corresponding section. Data were converted to mzXML format [25] using mzWiff (version 4.3.1, http://sourceforge.net/projects/sashimi/files/mzWiff%20(Analyst%20converter) with centroiding of MS1 and MS2 data, precursor charge determination, and deisotoping of MS2 data. Peptide sequences were identified by X! Tandem (version 2010.12.01) [27], including cyclic permutation, in conjunction with PeptideProphet (part of version 4.3.1 of the Trans Proteomic Pipeline) [15]. The same mouse proteome database as described in "quantitative proteome comparison" was used. Semi Arg-C specificity with up to three missed cleavage sites was applied. Static modifications are (+57.02 Da), lysine and N-terminal dimethylation (light formaldehyde + 28.03 Da; heavy formaldehyde + 34.06 Da). For acetylated N-termini (+42.01 Da), modifications are cysteine carboxyamidomethylation, N-terminal acetylation, and lysine dimethylation. Mass tolerance was 200 ppm for parent ions and 0.1 Da for fragment ions. X!Tandem results were further validated by PeptideProphet at a confidence level of >95 %. The relative quantification for each peptide was calculated using the ASAPratio [31] and XPRESS [33] algorithm as described for "Quantitative secretome comparison." Fc values are based on ASAPratio normalized for all peptide ratios. Two biological replicates with independent sample preparation (not the same samples as for quantitative proteome comparison) and mass spectrometric measurement were analyzed. In the first replicate, the first wild-type cell line was compared to the first Ctsb-deficient MEF cell line and in the second replicate the second wild-type MEF cell line was compared to the second Ctsb-deficient MEF cell line. Ratios were divided into the following quantiles: 0–20, 20–80, and 80–100 [36]. N-termini were considered as decreased if found in the quantile 0–20 in both biological replicates. Similarly, N-termini were considered as increased if found in the quantile 80–100 in both biological replicates.

LC–MS/MS analysis

For nanoflow-LC–MS/MS, TAILS samples were analyzed on a Qstar Elite (AB Sciex, Darmstadt, Germany) and samples for quantitative proteomic comparison on an Orbitrap XL (Thermo Scientific GmbH, Bremen, Germany) mass spectrometer. Both instruments were coupled to an Ultimate3000 micro pump (Thermo Scientific) with a flow rate of 300 nl/min each; 0.5 % acetic acid and 0.5 % acetic acid in 80 % acetonitrile (water and acetonitrile were at least HPLC gradient grade quality) with a gradient of increasing organic proportion were used for peptide separation. Column tips with 75-µm inner diameter and 11-cm length were self-packed [37] with Reprosil-Pur 120 ODS-3 (Dr. Maisch, Ammerbuch, Germany). The mass spectrometers were operated in the data-dependent mode and switched automatically between MS and MS/MS. For Qstar samples, the smart mode for MS/MS accumulation was used.

Western blot

Cell-conditioned media were prepared as described in "Quantitative secretome comparison" and concentrated using Microcon columns (regenerated cellulose 10000 MWCO; Millipore, Tullagreen, Carrigtwohill, Ireland). Protein content was determined using the Bradford method (Bio-Rad, Munich, Germany). Total cell extracts were prepared by on-plate lysis. Cells were washed twice with PBS and lysed by adding a lysis buffer containing 20 mM Tris-HCl (pH 7.5), 150 mM NaCl, 5 mM EDTA, and 1 % Triton X-100 and protease inhibitors (5 mM EDTA, 0.01 mM E64, 1 mM PMSF).

For secretome samples, reducing the sample buffer was added to 5 µg of protein and loaded onto 12 % SDS–polyacrylamide gels; 20–40 µg protein of total cell extract was loaded. Tubulin served as internal standard for total cell extract immunoblots. After electrophoretic separation, proteins were transferred on polyvinylidene fluoride (PVDF) membranes using a semidry blot system (BioRad, Munich, Germany). After blocking, the membranes were exposed to the primary antibodies [β-catenin 1:500, collagen α-1 (I) 1:5,000, Ctsb 1:500, Ctsl 1:500, Lamp-1 1:500; MMP-2 1:200; N-cadherin 1:1,000; periostin, 1:500; tubulin 1:1,000] overnight at 4 °C. After washing, the membranes were incubated for 2 h with the secondary antibody. Membranes were washed and developed with the West Pico Chemiluminescent substrate (Pierce, Rockford, IL, USA). Peroxidase activity was detected with a LumiImager device (Roche, Mannheim, Germany). Primary antibodies were purchased from Abcam (Lamp-1: catalog no. ab25245), BD Biosciences (β-catenin: catalog no. 610154), Acris Antibodies [collagen α-1 (I): catalog no. R1038X], Cell Signaling (N-cadherin: catalog no. #4061), Sigma Aldrich (tubulin: catalog no. T 6199), and R&D Systems, Minneapolis, MN, USA (Ctsb: catalog no. AF965; Ctsl: catalog no. AF1515; MMP-2: catalog no. AF1488; periostin: catalog no. AF2955). Western blots were quantified using the Fusioncapt advance software (Vilber Lourmat, Eberhardzell, Germany).

In vitro cleavage assays

CTSB and CTSL were stored in 50 mM sodium dihydrogen phosphate monohydrate, 50 mM sodium phosphate dibasic, 400 mM sodium chloride, and 5 mM EDTA at pH 6. CTSB and CTSL were activated by adding 2 mM DTT. Human MMP-2 (active site mutant; E404A) (50 ng/µl) and recombinant human CTSL (0.5 ng/µl) or CTSB (0.5 ng/µl), respectively, were incubated overnight at 37 °C in sodium acetate buffer (200 mM sodium acetate, 1 mM EDTA, 0.05 % Brij 35, pH 5.5), or sodium phosphate buffer (100 mM sodium phosphate, 0.4 M sodium chloride, 10 mM EDTA, pH 7). Samples were loaded onto 12 % SDS–polyacrylamide gels and bands visualized by silver staining.

Activation of pro-MMP-2

A 10-mM stock solution of p-aminophenylmercuric acetate (APMA) was prepared in 0.1 M NaOH. The stock solution was diluted in a buffer containing 25 mM Bis-Tris-HCl, 25 mM Tris-HCl, 100 mM NaCl, and 10 mM $CaCl_2$ to a concentration of 2.5 mM. Afterwards, pH was adjusted to 7.5. Recombinant murine pro-MMP-2 (R&D Systems, Minneapolis, MN, catalog no. 924-MP-010) was activated using 1 mM APMA and incubated for 3 h at 37 °C. The activated MMP-2 was passed over Microcon columns (regenerated cellulose 10000 MWCO; Millipore, Tullagreen, Carrigtwohill, Ireland) to remove APMA and low-molecular-weight impurities. Activated MMP-2 was added to the cell culture dish in a concentration of 125 ng/ml.

Results and discussion

Generation and characterization of cell lines

Wild-type, Ctsb-deficient, and Ctsb Ctsl double-deficient MEF cell lines were generated as described previously [22]. In total, two wild-type MEF cell lines, two $Ctsb^{-/-}$ MEF cell lines, and two $Ctsb^{-/-}Ctsl^{-/-}$ MEF cell lines were generated and polyclonally immortalized by viral transfection with the simian virus-40 large-T antigen (SV40) [24]. Afterwards, cells were controlled for cathepsin expression, proliferation, and alterations in morphology. SV40 immortalization does not affect cathepsin expression levels (Supplementary Fig. S1). All immortalized cell lines showed similar doubling times of 28–33 h (Supplementary Fig. S2A) and MEF prototypical morphology (data not shown).

An accumulation of lysosome-like organelles has been reported in heart and thyroid tissue as well as in keratinocytes and MEFs of Ctsl-deficient mice [22, 38–41]. The accumulation of cytoplasmic acidic vesicular structures was observed in both $Ctsb^{-/-}Ctsl^{-/-}$ MEF cell lines used in this study. Immunostaining for the lysosomal marker Lamp-1 in wild-type and $Ctsb^{-/-}Ctsl^{-/-}$ MEFs showed an accumulation of enlarged Lamp-1 positive vesicles in MEFs deficient for Ctsb and Ctsl (Fig. 1a). Accumulation was corroborated by immunoblotting for Lamp-1 (Supplementary Fig. S2B). Staining with the pH-sensitive fluorescent dye acridine orange revealed that the Lamp-1 positive vesicles are acidic (Fig. 1b). Interestingly, mice deficient for Ctsb and Ctsl develop autophagolysosomal and lysosomal accumulations in neurons, leading to neuronal cell death [15, 16], a phenotype not observed in single-deficient mice, but reflected in MEFs deficient for Ctsb and Ctsl. MEFs with single deficiency of Ctsb or Ctsl show a minor accumulation of acidic Lamp-1-positive vesicles compared to the prominent phenotype in Ctsb and Ctsl double-deficient MEFs.

Proteomic secretome analysis requires harvesting of cell conditioned media, which is obtained by growing cells to near confluence, followed by incubation in serum-free medium for 24 h [42–44]. To address whether serum starvation has different effects on wild-type and cathepsin-deficient cells, a lactate dehydrogenase (LDH) assay was performed and revealed similar cell viability of all cell lines independent of the genotype (Supplementary Fig. S2C).

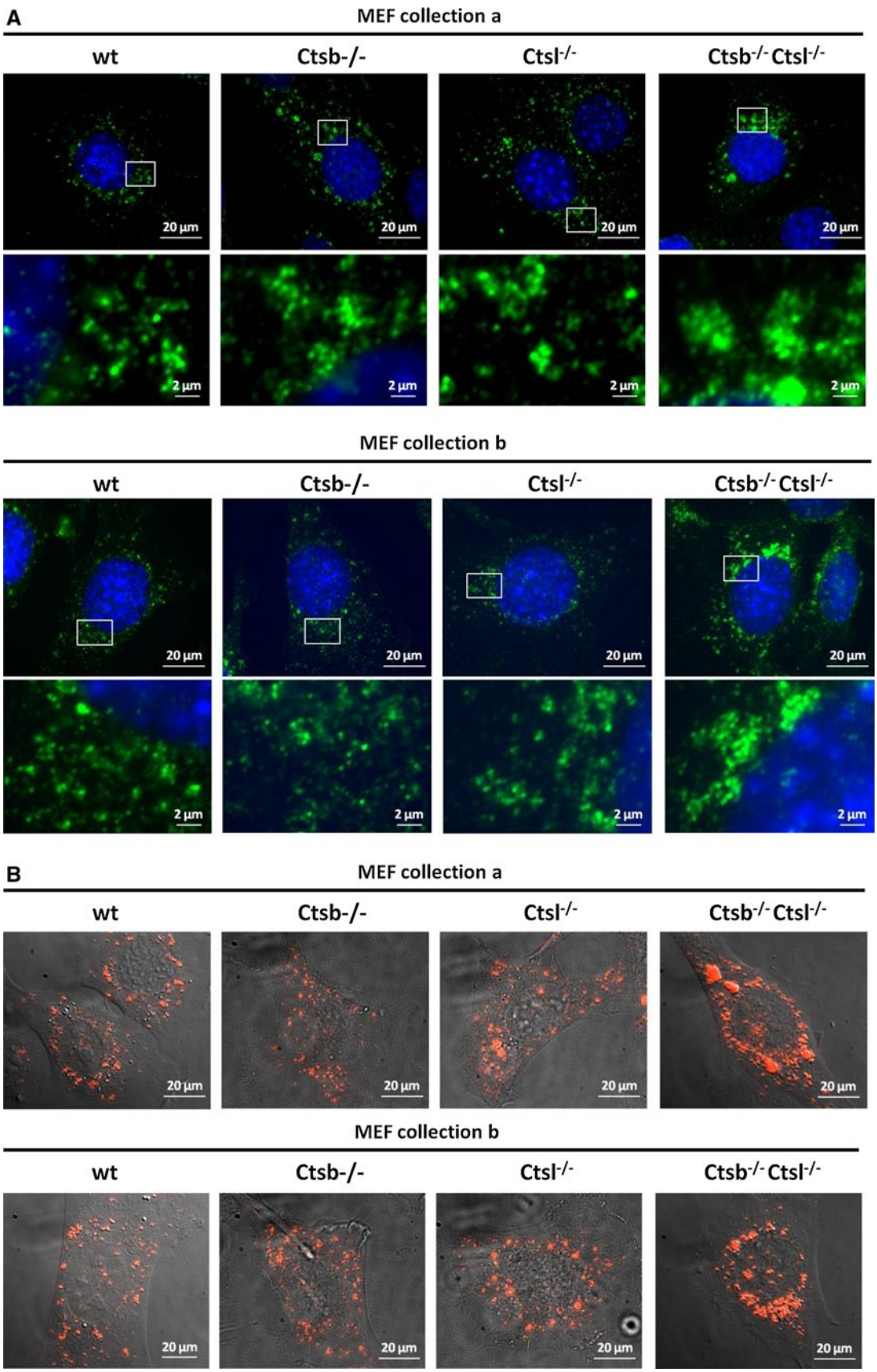
A
MEF collection a
wt
Ctsb-/-
Ctsl-/-
Ctsb-/- Ctsl-/-
20 µm
2 µm
MEF collection b
wt
Ctsb-/-
Ctsl-/-
Ctsb-/- Ctsl-/-
20 µm
2 µm
B
MEF collection a
wt
Ctsb-/-
Ctsl-/-
Ctsb-/- Ctsl-/-
20 µm
MEF collection b
wt
Ctsb-/-
Ctsl-/-
Ctsb-/- Ctsl-/-
20 µm

◂ **Fig. 1** Ctsb- and Ctsl-deficient MEFs, and to a lesser extent Ctsb single and Ctsl single-deficient MEFs, show accumulations of enlarged acidic Lamp-1-positive vesicles. **a** Immunofluorescent staining of two wild-type MEF cell lines, two Ctsb-deficient cell lines, two Ctsl-deficient cell lines, and two Ctsb Ctsl double-deficient MEF cell lines with the lysosomal marker Lamp-1 (*green*). Nuclei are stained with Hoechst (*blue*). **b** Visualization of acidic vesicles with acridine orange staining

Hence, wild-type and cathepsin-deficient cell lines are highly comparable for proteomic analysis.

Here we demonstrate that double deficiency of Ctsb and Ctsl in MEFs results in accumulation of enlarged acidic Lamp-1 positive vesicles, which does not affect cell viability or morphology. Since Ctsb and Ctsl single-deficient MEFs display minor lysosomal accumulations, this further supports the hypothesis of collaborative functionality between both cathepsins and generates interest as to how Ctsb and Ctsl double deficiency affects proteome composition. A previous study demonstrated a prominent effect of Ctsl on secretome composition [13]. To elucidate first the impact of Ctsb alone on the extracellular proteome, we started with a quantitative proteome comparison of wild-type and Ctsb-deficient MEFs.

Effect of Ctsb depletion on protein abundance

To elucidate the impact of Ctsb on secretome composition, we quantitatively compared cell-conditioned media (CCM) of wild-type MEFs and MEFs deficient for Ctsb. Each proteomic analysis was performed in biological replicates, comparing the first Ctsb-deficient MEF cell line with the first wild-type MEF cell line and the second Ctsb-deficient MEF cell line with the second wild-type MEF cell line. For proteomic analysis, stable isotope labeling with either d(2)^{13}C-formaldehyde ("heavy") or d(0)^{12}C formaldehyde ("light") in combination with liquid chromatography—tandem mass spectrometry (LC–MS/MS) was employed. Comparison of the secretome of wild-type MEFs and MEFs deficient for Ctsb identified 1,562 proteins in the first biological replicate (replicate 1) (Supplementary Table S1) and 1,718 proteins in the second biological replicate (replicate 2) (Supplementary Table S2). A total of 1,363 proteins were identified in both biological replicates (Fig. 2a). Of these, ~25 % were annotated as secreted or extracellularly localized using the Gene Ontology database (GO) or Swissprot annotation. This percentage corresponds well to published secretome analyses [43, 45]. Alterations of protein abundances are stated as fold change values [Fc; $\log_2$ of the heavy/light (H/L) ratio]. The distribution profiles of Fc values for all identified proteins in both biological replicates showed a near normal distribution (Supplementary Fig. S3A/B) and an average Fc close to zero (Fig. 2b).

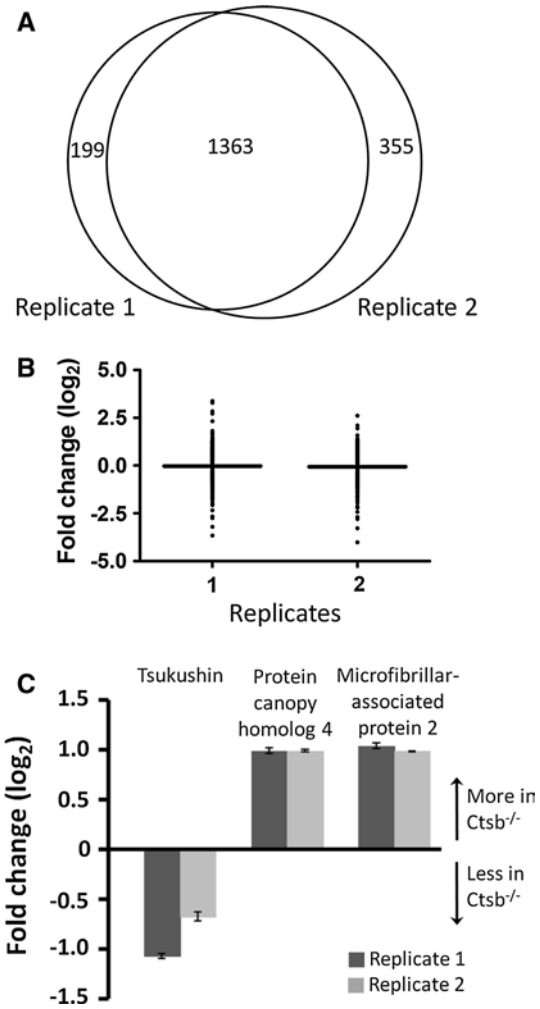

Fig. 2 Protein identification and quantification for each biological replicate of the quantitative secretome: comparison of wild-type and Ctsb-deficient cell-conditioned media. **a** In both biological replicates 1,363 proteins were identified, whereas 199 and 355 proteins were found only in the first or the second replicate, respectively. **b** Distribution and geometric mean (*horizontal bar*) of fold change values ($\log_2$) of proteins from each replicate comparing the wild-type and *Ctsb*$^{-/-}$ MEF secretome. **c** Proteins with significantly altered protein abundance. These proteins are identified in both biological replicates, display an ASAPratio *p* value lower than 0.1 (indicated by *arrow bars*), show an alteration in abundance of more than 50 % (Fc < −0.58; Fc > 0.58) in both replicates (*dark grey bars*, replicate 1; *light grey bars*, replicate 2), and are annotated as secreted or extracellularly localized according to GO or Swissprot annotation

Proteins were considered to be significantly altered in their abundance if they were identified in both biological replicates, displayed an ASAPratio *p* value lower than 0.1 in each replicate, showed an alteration in abundance of more than 50 % (Fc < −0.58; Fc > 0.58) in both replicates, and were annotated as secreted or extracellularly localized using the GO or Swissprot annotation. An ASAPratio *p* value cutoff of 0.1 was suggested by the original ASAPratio

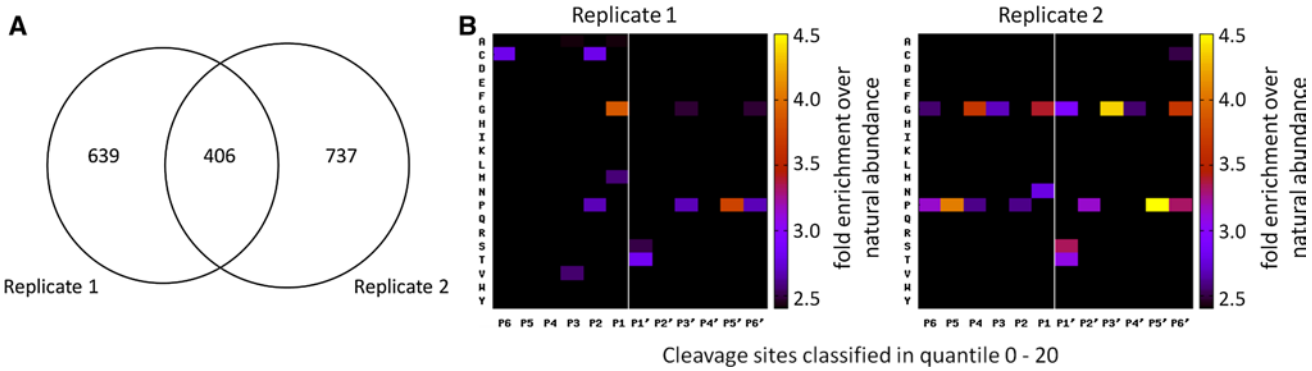

Fig. 3 N-terminal peptides identified and quantified for each biological replicate in the TAILS experiment comparing wild-type and Ctsb-deficient cell-conditioned media. **a** Four hundred six peptides (naturally unmodified, chemically dimethylated N-termini) were identified in both biological replicates. **b** Global specificity pattern upon Ctsb ablation. Graphical presentation of the secretome specificity profile of all N-termini found in the 0–20 quantile and therefore decreased upon Ctsb deletion. Only N-termini annotated as secreted or extracellularly localized according to GO or Swissprot annotation were considered. Positional occurrences are shown as enrichment over natural abundance of murine amino acid abundances as derived from the International Protein Index [74]. TAILS identifies prime-site sequences of proteolytic cleavage sites. The corresponding non-prime sequences are derived bioinformatically by database searches similar to the PICS strategy for protease specificity characterization [52, 54]

publication [31]. Tsukushin, protein canopy homolog 4, and microfibrillar-associated protein 2 fulfilled these strict criteria (Fig. 2c). Numerous proteins were altered in abundance in either the first or second biological replicate. For instance, secreted frizzled-related protein 1 (SFRP-1), interleukin-1 receptor-like 1, C-X-C motif chemokine 5, and periostin displayed altered protein abundance only in one replicate. The low number of proteins affected in both replicates illustrates nicely the intrinsic biological variability and highlights the importance of true biological replicates as done in this study.

Cathepsins D, K, L, O, Z, legumain, as well as the cysteine protease inhibitors cystatin B and C were identified in both biological replicates, but displayed only minor abundance alteration (Supplementary Table S1/2). Overall, Ctsb has a very limited effect on secretome composition. Similarly, in murine skin, Ctsl has a stronger impact on proteome composition compared to Ctsb [14].

Identification of Ctsb-dependent cleavage events by TAILS

Proteolytic processing is a tightly regulated process that affects every protein through either limited proteolysis or terminal degradation [46]. Limited proteolysis yields stable cleavage products with new N- and C-termini and often altered functionality. To elucidate how Ctsb contributes to extracellular proteolysis and the secretome cleavage pattern in the MEF secretome, we applied the quantitative N-terminomic technique TAILS [20, 47]. TAILS allows for quantification of protein N-termini from different biological samples. Here, CCM of wild-type MEFs and Ctsb-deficient MEFs were compared. Previously, TAILS was employed in a secretome cleavage analysis comparing MEFs deficient for Ctsl to wild-type MEFs [13]. The TAILS workflow follows a negative selection procedure in which naturally unmodified as well as naturally modified (e.g., acetylated) N-termini are identified and quantified. Naturally unmodified protein N-termini possess primary amines ($–NH_2$) and comprise native as well as proteolytically generated protein N-termini. All naturally unmodified protein N-termini, which in most cases represent sites of proteolytic processing, are chemically dimethylated using isotopically labeled formaldehyde.

TAILS was performed in two biological replicates comparing the secretome of wild-type MEFs and Ctsb-deficient MEFs. Thereby, TAILS identified 1,045 naturally free (chemically dimethylated) protein N-termini in the first biological replicate (Supplementary Table S3) and 1,143 naturally free (chemically dimethylated) protein N-termini in the second biological replicate (Supplementary Table S4) with an overlap of 406 naturally free (chemically dimethylated) protein N-termini identified in both biological replicates (Fig. 3a).

To distinguish quantitatively unaltered protein N-termini from N-termini displaying an alteration in abundance, we chose a quantile-based approach as described in experimental procedures. Quantitatively fewer abundant protein N-termini in Ctsb-deficient cells represent possible Ctsb-dependent cleavage events. Based on these criteria, we quantified 205 protein N-termini in the first replicate (TAILS) (Supplementary Table S5) and 227 protein N-termini in the second replicate (TAILS) (Supplementary Table S6) as less abundant in the Ctsb-deficient MEF secretome. Of these, 24 protein N-termini were underrepresented in

the Ctsb-deficient secretome in both biological replicates and annotated as secreted or extracellular localized using the GO database or Swissprot annotation (Table 1). This small number reflects the result of the quantitative proteome comparison of wild-type and Ctsb-deficient MEFs, where a limited effect of Ctsb on secretome composition is observed. In contrast, Ctsl had a more pronounced effect on cleavage events in the secretome [13].

Included in this list are cleavage events in collagen α-1 (I) and collagen α-2 (I). Overall protein abundances of both proteins were unaffected upon Ctsb depletion (Supplementary Tables S1/2), which was further confirmed for collagen α-1 (I) by immunoblotting (Fig. 5). Several additional cleavage sites in collagen α-1 (I) and collagen α-2 (I), but also other collagens, were identified in either the first or the second biological replicate. Moreover, a Ctsb-dependent cleavage site was identified in both biological replicates for fibronectin and in the first leucine-rich repeat of biglycan. Cleavage of collagens as well as fibronectin by Ctsb has been reported before [48–50], underlining the important role of Ctsb in extracellular matrix (ECM) remodeling, a crucial step in the process of tumor cell invasion [10, 51].

Sometimes altered abundance of an N-terminus is best explained by overall altered protein abundance. This is the case for extracellular superoxide dismutase and the matricellular protein periostin. Extracellular superoxide dismutase was quantified less abundantly in the first replicate in the quantitative proteome comparison upon Ctsb deficiency (Supplementary Table S1), and periostin was quantified less abundantly in the second replicate (Supplementary Table S2). A decrease of periostin was corroborated by immunoblotting (Fig. 5). Hence, altered abundance of the corresponding N-termini may reflect altered protein abundance rather than impaired proteolytic processing.

For insulin-like growth factor-binding protein (IGFBP)-3 and IGFBP-6, we detected quantitatively decreased cleavage sites corresponding to removal of signal peptides (Table 1). We consider this to be indicative of decreased protein abundance rather than decreased activity of the signal peptidase. In fact, IGFBP-6 was quantified less abundantly upon Ctsb deficiency in both biological replicates of the quantitative proteome comparison [Fc (first replicate) $= -0.17$, Fc (second replicate) $= -0.43$].

N-terminomic analysis of Ctsb-deficient skin revealed that Ctsb represents an important node in the protease web [14], thereby affecting the abundance of several proteases and their inhibitors. To investigate whether the majority of affected cleavage events represent proteolytic processing by Ctsb or further proteases, we analyzed the secretome cleavage pattern upon Ctsb deficiency. Since TAILS identifies the prime-site sequence of proteolytic cleavage sites, the corresponding non-prime sequences are derived bioinformatically using a strategy established for the proteomic identification of protease cleavage sites (PICS) [52–54]. The global cleavage pattern of all underrepresented cleavage sites upon Ctsb deficiency is shown in Fig. 3b. Cleavage patterns of both biological replicates are highly reproducible, which was observed before for cleavage patterns of the Ctsl-deficient secretome and for the Ctsb as well as the Ctsl-deficient skin proteome [13, 14]. This illustrates nicely the robustness of the TAILS technique.

In vitro, Ctsb specificity is defined by a strong preference for a glycine residue in P3′ position and for aromatic residues in P2 position [55]. The preference for glycine residues in P3′ is reflected by the secretome cleavage pattern of the second replicate and to a lesser extent also of the first replicate. However, the preference for aromatic residues in P2 is not observed in the secretome cleavage pattern, indicating a mixture of primary Ctsb-catalyzed cleavage events and "overshadowing" indirect, downstream proteolysis. In striking contrast, Ctsl deficiency alone resulted almost exclusively in "overshadowing" indirect, downstream proteolytic events. At the same time, deficiency of either cathepsin led to a prominent footprint on extracellular cleavage events.

Secretome analysis of Ctsb and Ctsl double-deficient MEFs

Cysteine cathepsins functionally cooperate with deficiency of one cysteine cathepsin being compensated by other cathepsins, as has been shown for Ctsb and cathepsin Z (Ctsz) [56, 57]. Compensatory function can be suggested for Ctsb and Ctsl as well, since Ctsb, together with Ctsz and cathepsin D (Ctsd), is more abundant in Ctsl-deficient skin [14]. A decrease of Ctsd in Ctsl-deficient skin is probably caused by diminished degradation, since Ctsl contributes significantly to Ctsd degradation [58]. Mice deficient in Ctsb and Ctsl develop autophagolysosomal and lysosomal accumulations in neurons, leading to neuronal cell death in the cerebral cortex and a degeneration of cerebellar Purkinje and granule cells, with eventual death of these mice 4 weeks after birth [15, 16]. Single-gene-deficient mice for Ctsb or Ctsl do not show lysosomal storage disorders, substantiating mutual compensation between Ctsb and Ctsl and a shared substrate pool in vivo [15, 17].

To address whether alterations in secretome composition potentiate upon Ctsb and Ctsl double deletion, a quantitative proteome comparison was performed comparing the CCM of Ctsb and Ctsl double-knockout MEFs to wild-type MEFs. Like for the analysis of the Ctsb-deficient MEF secretome, two biological replicates were performed, and stable isotope labeling with differentially labeled formaldehyde in combination with LC–MS/MS was employed. In the first replicate 2,173 proteins (Supplementary Table S7) and in the second replicate 2,352 proteins were identified

Table 1 List of all naturally unmodified (chemically dimethylated) N-termini (a) annotated as secreted or extracellularly localized using the Gene Ontology database (GO) or Swissprot annotation and (b) found in the 0–20 quantile upon Ctsb deletion in both biological replicates

Uniprot	Protein	Fold change (log_2 of $Ctsb^{-/-}$/wt ratio) in replicate 1	FC-error in replicate 1	Fold change (log_2 of $Ctsb^{-/-}$/wt ratio) in replicate 2	FC-error in replicate 2	Non-prime sequence (from database)	Prime sequence (experimentally determined)
PGS1_MOUSE	Biglycan	−0.52	0.04	−1.76	0.30	KTVPKEISPD	T_{93}TLLDLQNNDISELR
C01A1_M0USE	Collagen alpha-1(I) chain	−0.60	0.04	−0.91	0.19	GPPGPAGAPG	D_{769}KGEAGPSGPPGPTGAR
C01A1_M0U5E	Collagen alpha-1(I) chain	−2.16	0.19	3.17	0.86	FCPEEYVSPN	S_{95}EDVGVEGPKGDPGPQGPR
C01A1_M0USE	Collagen alpha-1(I) chain	−0.79	0.03	−2.48	0.56	GAKGEPGATG	V_{445}QGPPGPAGEEGKR
C01A2_MOUSE	Collagen alpha-2(I) chain	−0.63	0.02	−1.13	0.10	NKAVLLQGSN	D_{1303}VELVAEGNSR
C01A2_M0USE	Collagen alpha-2(I) chain	−0.96	0.04	−2.13	0.19	GEQGPAGPPG	F_{600}QGLPGPSGTTGEVGKPGER
C01A2_MOUSE	Collagen alpha-2(I) chain	−3.66	0.46	−6.38	0.00	PGIAGALGEP	G_{901}PLGISGPPGAR
C01A2_M0USE	Collagen alpha-2(I) chain	−0.47	0.06	−2.02	0.65	HGNRGEPGPA	G_{991}SVGPVGAVGPR
SODE_MOUSE	Extracellular superoxide dismutase [Cu–Zn]	1.72	0.23	−1.27	0.31	LAACGSVTMS	N_{21}PGESSFDLADR
FINC_MOUSE	Fibronectin	−0.93	0.05	−1.82	0.26	EWKCERHALQ	S_{278}ASAGSGSFTDVR
LEG1_MOUSE	Galectin-1	−0.60	0.06	−1.39	0.36	MACG	L_5VASNLNLKPGECLKVR
LEG1_MOUSE	Galectin-1	−0.66	0.05	−0.97	0.13	PRFNAHGDAN	T_{58}IVCNTKEDGTWGTEHR
GELS_MOUSE	Gelsolin	−1.72	0.11	−0.93	0.16	KNWRDPDQTD	G_{353}PGLGYLSSHIANVER
GRIA2_MOUSE	Glutamate receptor 2	−4.68	0.00	−6.38	0.00	ADQEYSAFRV	G_{47}MVQFSTSEFR
HSP7C_MOUSE	Heat shock cognate 71 kDa protein	−1.55	0.05	−4.35	0.89	FTDTERLIGD	A_{55}AKNQVAMNPTNTVFDAKR
Q6PE62_MOUSE	Insulin-like growth factor binding protein 3	−2.16	0.19	−2.17	0.49	LLRGPPVARA	G_{28}AGAVGAGPWR
Q91X24_MOUSE	Insulin-like growth factor-binding protein 6	−1.44	0.20	−1.92	0.58	FAAGSGSALA	G_{29}CPGCGAGMQTGCR
Q91X24_MOUSE	Insulin-like growth factor-binding protein 6	−1.16	0.13	−1.79	0.43	LLFAAGSGSA	L_{27}AGCPGCGAGMQTGCR
LRP8_MOUSE	Low-density lipoprotein receptor-related protein 8	−1.00	0.10	−0.95	0.13	LLLQLQHLSA	A_{28}DPLPGGQGPVKECEEDQFR
OLM2A_MOUSE	Olfactormedin-like protein 2A	0.89	0.03	−0.83	0.13	VLLRAGPVWP	D_{33}SKVFSDLDQVR
POSTN_MOUSE	Periostin	−0.55	0.02	−1.88	0.14	PIIKTEGPAM	T_{703}KIQIEGDPDFR
POSTN_MOUSE	Periostin	−1.20	0.11	−2.02	0.33	AVMPIDHVYG	T_{106}LGIVGATTTQHYSDVSKLR
PDIA3_M0USE	Protein disjlfide-isomerase A3	−1.44	0.04	−2.21	0.31	SGYPTLKIFR	D_{85}GEEAGAYDGPR
UBP14_MOUSE	Ubiquitin carboxyl-terminal hydrolase 14	−3.66	0.00	−5.01	0.00	GALRASGEMA	S_{113}AQYITAALR

Non-prime sequences were derived by database search

(Supplementary Table S8); 1,826 proteins were identified in both biological replicates (Fig. 4a). Of these, ~30 % were annotated as secreted or extracellularly localized using the GO or Swissprot annotation. This percentage corresponds well to published CCM proteomic data [43, 45]. The distribution profiles of Fc values for all identified proteins in both biological replicates revealed a normal distribution (Supplementary Fig. S3C/D) and an average Fc close to zero (Fig. 4b).

Numerous protein alterations highlight the cooperative functionality of Ctsb and Ctsl

To address whether overall more proteins are affected upon Ctsb and Ctsl depletion, we determined the proportion of proteins affected upon single deficiency of either Ctsb or Ctsl and double deficiency. Upon Ctsb and Ctsl depletion, a decrease or increase of protein abundance by more than 50 % (Fc < −0.58; Fc > 0.58) is observed for 29 % (640 proteins) of all identified proteins in the first replicate and for 31 % (726 proteins) of all identified proteins in the second replicate. This percentage of altered proteins exceeds the number of altered proteins observed from proteome comparisons of Ctsb single-deficient or Ctsl single-deficient MEFs and mirrors the strong impact of a combined loss of Ctsb and Ctsl on the MEF secretome composition. Of all identified proteins, 16–17 % were altered by more than 50 % in the Ctsb-deficient MEF secretome. Similarly, 19–21 % of all identified proteins were altered by more than 50 % in a study comparing the secretome of wild-type and Ctsl-deficient MEFs [13].

Cutoff at a certain Fc value alone serves for a global overview. However, to identify individual proteins as significantly affected by Ctsb and Ctsl depletion, we chose strict criteria as previously described for the secretome analysis of Ctsb-deficient MEFs. Of the 49 proteins

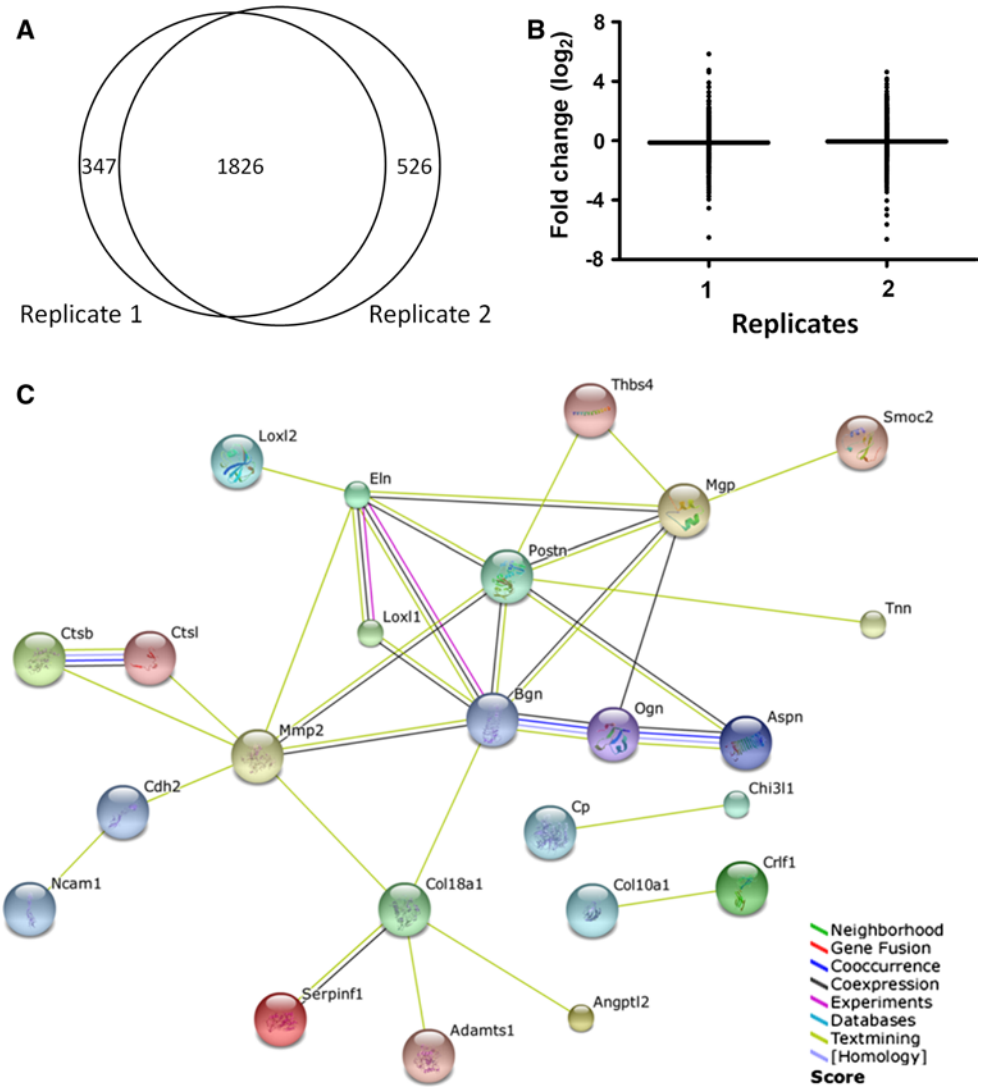

Fig. 4 **a** A total of 1,826 proteins were identified in both biological replicates of the quantitative proteome comparison of wild-type and Ctsb Ctsl-deficient cell-conditioned media. **b** Distribution and geometric mean (*horizontal bar*) of fold change values (log_2) of proteins from each replicate comparing the wild-type and $Ctsb^{-/-}$ $Ctsl^{-/-}$ MEF secretome. **c** Overall connectivity of all extracellular and secreted proteins altered in the quantitative proteome comparison of wild-type and Ctsb Ctsl-deficient MEFs determined by STRING (Search Tool for the Retrieval of Interacting Genes/Proteins). *Different line colors* represent the types of evidence for each association

fulfilling these strict criteria, collagen α-1 (XII), cochlin, glia-derived nexin (serpine E2), MMP-2, periostin, and tenascin-N were also affected by Ctsl deficiency alone [13]. However, the majority of proteins altered upon Ctsb and Ctsl double deficiency were not significantly affected in cathepsin single-deficient cells, for either Ctsb or Ctsl. This strongly highlights cooperative activity of both proteases while simultaneously illustrating a prominent contribution of lysosomal proteases to extracellular proteome composition.

Biological processes affected by Ctsb and Ctsl depletion: cell adhesion and signaling

To identify interactions between all altered proteins in the Ctsb- and Ctsl-deficient secretome (Table 2), we employed the online resource Search Tool for the Retrieval of Interacting Genes (STRING) [59]. STRING unravels links between proteins based on published literature and large-scale databases. STRING found connectivity between affected proteins and placed MMP-2, biglycan, and periostin at the core (Fig. 4c). Additionally, STRING depicted shared biological processes of these proteins (Supplementary Fig. S4). Many proteins affected by ablation of Ctsb and Ctsl were involved in "Cell adhesion" and "Biological adhesion" (classification according to Gene Ontology, GO). Among others, periostin, tenascin-N, SPARC-related modular calcium-binding protein 2, thrombospondin-4, and cell growth regulator with EF hand domain protein 1 were quantified less abundantly, whereas neural cell adhesion molecule 1 (NCAM-1) and cadherin-2 (N-cadherin) were quantified more abundantly in the Ctsb- and Ctsl-deficient secretome. Higher abundance of N-cadherin in the secretome represents increased cell-associated N-cadherin levels, since immunoblotting corroborated higher protein levels for N-cadherin in the secretome as well as in total cell lysates (Fig. 5a/Supplementary Fig. S5A).

Another biological process affected by Ctsb and Ctsl ablation is "regulation of response to stimulus" (GO classification) (Supplementary Fig. S4) with a strong impact on the Wnt signaling pathway. The Wnt signaling pathway represents one of a few key molecular cascades that determine the cell fate in animals throughout their lifespan [60]. Wnt signaling can be inhibited by downregulation of Wnt ligands or by secreted Wnt inhibitors belonging to the family of Secreted Frizzled-Related Proteins (sFRPs) [61]. SFRP-1 and sFRP-2 abundance was highly affected upon Ctsb and Ctsl ablation, albeit in different directions: SFRP-1 was more abundant and sFRP-2 was less abundant in the Ctsb- and Ctsl-deficient secretome (Table 2). In the canonical Wnt cascade, β-catenin is the key effector responsible for transduction of the signal to the nucleus, where it associates with the T-cell factor/lymphocyte enhancer factor (TCF/LEF) transcription factors and drives the transcription of Wnt/β-catenin target genes [60], like sFRP-1 [62]. Interestingly, β-catenin was more abundant in the total cell lysate (Supplementary Fig. S5B) of Ctsb- and Ctsl-deficient MEFs, substantiating the observation that Wnt signaling is affected by Ctsb and Ctsl depletion.

Differential regulation of SFRPs indicates a specific effect of Ctsb and Ctsl double deficiency rather than global proteome rearrangement.

Ctsb and Ctsl double depletion strongly affects matricellular proteins and ECM components

STRING analysis further revealed an association of many proteins showing altered protein levels upon Ctsb and Ctsl depletion with "extracellular matrix organization" (Supplementary Fig. S4). Among these are several structural ECM or basement membrane (BM) proteins such as members of the collagen family; collagen α-1 (X), collagen α-1 (XII), and collagen α-1 (XVIII) were all less abundant, which was corroborated for collagen α-1 (I) by immunoblot analysis (Fig. 5). The important role of Ctsb in ECM composition is underlined by TAILS data, which revealed a number of Ctsb-dependent cleavage events in ECM proteins (Table 1; Supplementary Table S3/4). Laminins are glycoproteins that are located in the BM and able to bind to collagens. Laminin was reported to be degraded by Ctsb [63]. We quantified the laminin subunit beta-2 to be less abundant upon Ctsb and Ctsl double depletion. Moreover, elastin displayed lower abundance upon Ctsb and Ctsl depletion. Interactions between elastin and Ctsl or cathepsin K, which was quantified less abundantly, have been shown before [64].

The quantitative proteome comparison revealed strongly reduced protein levels of the matricellular protein periostin upon Ctsb and Ctsl deficiency. Periostin mediates cancer stem cell maintenance and metastatic dissemination by facilitating increased Wnt signaling [65] and directly interacts with other ECM proteins such as collagen type I, collagen type V, fibronectin, and tenascin-N [66]. In line with these data, periostin knockout mice show abnormalities in collagen fibrillogenesis leading to increased skin stiffness and decreased skin elasticity [67]. In Ctsl-deficient skin, periostin protein accumulates, over-writing a transcriptional downregulation [14]. In cultured MEFs, both Ctsl and, to a larger extent, Ctsb regulate periostin levels. Double deficiency results in a drastic decrease of periostin levels (Fig. 5), showcasing the cooperative effect of B and L.

Together, the three studies establish a novel yet strong link between cathepsins B and L and periostin.

Table 2 List of all extracellular and secreted proteins displaying altered protein abundance in the quantitative secretome comparison of wild-type and Ctsb Ctsl-deficient MEFs (right columns)

WT/Ctsb$^{-/-}$ replicates		Protein name	WT/Ctsb$^{-/-}$Ctsl$^{-/-}$ replicates	
1	2		1	2
0.03	-0.22	Angiopoietin-related protein 2	-1.40*	-2.37*
0.27	-0.05	Asporin	-3.20*	-2.91*
0.08	-0.26	A disintegrin and metalloproteinase with thrombospondin motifs 1; ADAMTS-1	-0.94*	-1.71*
0.07	0.07	Cadherin-2; N-Cadherin	1.09*	1.73*
0.11	-0.03	Cathepsin K	-1.48*	-3.30*
n.d.	n.d.	Ceruloplasmin	2.0*	2.95*
1.249*	-0.05	Cell growth regulator with EF hand domain protein 1	-1.00*	-1.61*
-0.37	-0.24	Chitinase-3-like protein 1	-0.85*	-1.37*
n.d.	n.d.	Collagen alpha-1(X) chain	-3.35*	-2.44*
0.16	-0.624*	Collagen alpha-1(XII) chain	-1.72*	-2.22*
-1.14*	0.52	Cochlin	-3.20*	-3.44*
0.71	-0.17	Collagen alpha-1(XVIII) chain	-2.94*	-2.81*
-0.53	0.21	Cytokine receptor-like factor 1	-1.36*	-3.30*
-0.49	-0.82	C-X-C motif chemokine 5	-2.62*	-2.44*
0.65	-0.58	Protein Col6a3	-2.35*	-1.71*
3.29*	0.59	Elastin	-0.97*	-1.40*
0.41	-0.84*	Glia-derived nexin; Serpin E2	-2.20*	-3.16*
-0.28	n.d.	Golgi apparatus protein 1	-1.03*	-1.00*
-0.25	0.09	Insulin-like growth factor-binding protein 4	1.38*	1.40*
-0.17	-0.58*	Leukocyte elastase inhibitor A; Serpin B1	-0.97*	-2.30*
0.08	0.65*	Interleukin-1 receptor-like 1	-1.10*	-3.30*
0.81	-0.37	Laminin subunit beta-2	-2.00*	-2.09*
0.42	0.14	Lysyl oxidase homolog 1	-1.07*	-1.00*
0.55	n.d.	Lysyl oxidase homolog 2	2.26*	2.27*
0.39	-0.41	Mannan-binding lectin serine protease 1	-1.20*	-2.29*
0.00	-0.96*	Matrix Gla protein	-1.57*	-1.29*
0.44	-0.62	Mimecan	-1.57*	-1.76*
1.02	0.88*	MMP-2; 72 kDa type IV collagenase	1.24*	2.72*
n.d.	-1.21	Neural cell adhesion molecule 1; NCAM-1	1.87*	2.06*
1.17*	-0.26	Protein NOV homolog; Insulin-like growth factor-binding protein 9	-1.20*	-1.22*
0.26	-0.74	Lysosomal Pro-X carboxypeptidase	-0.97*	-0.94*
0.54	0.32	Platelet-derived growth factor D	-2.35*	-2.53*
0.45	-0.19	Pigment epithelium-derived factor	-1.07*	-1.00*
0.24	-0.22	Proenkephalin-A	-1.88*	-5.01*
0.58	0.00	Biglycan	-1.52*	-0.97*
0.96*	-0.88*	Periostin	-2.94*	-4.61*
n.d.	n.d.	Poliovirus receptor-related protein 2	1.99*	1.61*
-1.14	n.d.	Secreted frizzled-related protein 1	2.47*	2.90*
1.12*	-0.08	Secreted frizzled-related protein 2	-3.06*	-2.62*
-0.36	-0.17	SPARC-related modular calcium-binding protein 2	-1.40*	-1.49*
0.70	-0.03	Sushi, nidogen and EGF-like domain-containing protein 1	-1.13*	-2.81*
0.41	-0.62*	Scavenger receptor cysteine-rich domain-containing protein LOC284297 homolog	-1.57*	-1.06*
-0.09	0.39	Extracellular sulfatase Sulf-1	-1.10*	-1.22*
0.55	-0.51	Sushi, von Willebrand factor type A, EGF and pentraxin domain-containing protein 1	-1.94*	-3.29*
0.07	-0.16	Tenascin-N	-3.20*	-3.16*
0.84	0.21	Tetranectin	-2.83*	-2.44*
-0.51	n.d.	Tissue factor pathway inhibitor	1.73*	1.71*
n.d.	-0.41	Testican-2	-1.43*	-0.83*
0.57	-0.21	Thrombospondin-4	-2.94*	-4.04*

Fold change (log_2 value)	
less in Cts$^{-/-}$	≤ -1.59
	-1.58 to -0.59
no change	-0.58 to 0.58
	0.59 to 1.58
more in Cts$^{-/-}$	> 1.59

All proteins (a) are annotated as secreted or extracellularly localized according to GO or Swissprot annotation, (b) display a ASAPratio p value lower than 0.1 in both biological replicates and (c) show an alteration in abundance by more than 50 % (Fc < −0.58; Fc > 0.58) in both replicates. For comparison protein fold changes of the quantitative secretome comparison of wild-type and Ctsb deficient MEFs are shown (left columns). Fold change values were calculated based on protein ratios Ctsl$^{-/-}$/wild-type. Background colors indicate magnitude of protein alteration

nd no data

* p value <0.1

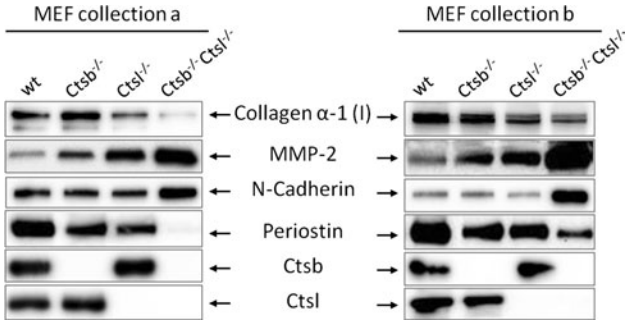

Fig. 5 Western blot analysis of cell-conditioned media of wild-type, Ctsb-deficient, Ctsl-deficient, and *Ctsb*$^{-/-}$ *Ctsl*$^{-/-}$ MEFs for collagen α-1 (I), MMP-2, N-cadherin, and periostin. Absence of Ctsb and/or Ctsl was controlled by detection of the Ctsl and Ctsb proform

Deletion of Ctsb and Ctsl results in altered abundance of proteases and protease inhibitors

Ablation of Ctsb or Ctsl has a pronounced effect on protein abundance of several proteases and protease inhibitors, characterizing both cathepsins as important regulatory modules in the proteolytic network [14]. This has been corroborated by the Ctsl-deficient secretome cleavage pattern of MEFs [13] and to some extent by the Ctsb-deficient secretome cleavage pattern (Fig. 2b). This finding is further highlighted by protein alterations of proteases and their inhibitors in the Ctsb- and Ctsl-deficient secretome. These include alterations of several serine protease inhibitors such as glia-derived nexin (serpin E2), leukocyte elastase inhibitor A (serpin B1), and tissue factor pathway inhibitor (Table 2). Protein levels of glia-derived nexin were altered upon deficiency of Ctsl alone [13], hence representing a process independent of Ctsb.

Whereas the cysteine protease inhibitor cystatin B was not altered, cystatin C levels are decreased upon Ctsb and Ctsl depletion in both biological replicates, albeit not entirely fulfilling our cutoff criteria. Ctsd and legumain displayed only a slight decrease in both biological replicates upon Ctsb and Ctsl double depletion. The proteases mannan-binding lectin serine protease 1, cathepsin K, and a disintegrin and metalloproteinase with thrombospondin motifs (ADAMTS)-1 were strongly reduced in abundance in the Ctsb and Ctsl-depleted secretome (Table 2). Protein levels of ADAMTS-1 were not affected upon sole removal of Ctsb (Table 2) or Ctsl [13], pointing to a cooperative role of Ctsb and Ctsl in regulation of ADAMTS-1 protein abundance.

MMP-2 abundance was increased upon Ctsb and Ctsl double deficiency (Table 2). Its expression and activity are upregulated in numerous types of cancer and correlate with elevated metastasis and poor prognosis [68–70]. Altered protein levels of MMP-2 upon single Ctsb and Ctsl depletion were confirmed by immunoblotting, revealing a stronger increase of MMP-2 upon Ctsl deficiency compared to Ctsb (Fig. 5). A more drastic alteration in MMP-2 abundance was observed upon Ctsb and Ctsl double depletion. Increase of MMP-2 protein levels is a very robust phenomenon. It occurs equally for cells grown on top of fibronectin or collagen IV. Furthermore, the MMP-2 increase is independent from amino acid starvation. (Supplementary Fig. S6). This is underlined by an accumulation of MMP-2 in primary Ctsl-deficient MEFs as well as upon treatment of wild-type MEFs with the cysteine cathepsin inhibitor E64d (Fig. 6a, b).

Ctsl re-expression rescues MMP-2 abundance and indicates a degradative Ctsl-MMP-2 axis

Since Ctsl deficiency alone already affects MMP-2 protein levels, we re-expressed Ctsl in Ctsl-deficient MEFs and mildly overexpressed Ctsl in wild-type MEFs. A bicistronic retroviral expression system was applied to gain polyclonal, stable, and dosable Ctsl expression. Re-expression of Ctsl in *Ctsl*$^{-/-}$ MEFs and wild-type MEFs led to a decrease of MMP-2, underlining a strong impact of Ctsl on MMP-2 expression (Fig. 6c). Since it has been shown that Ctsl does not affect gene expression, activation, or secretion of MMP-2 [13], impaired MMP-2 degradation could explain its increased protein levels upon Ctsl depletion. To test if Ctsl itself has the ability to degrade MMP-2, we performed in vitro cleavage assays using an MMP-2 active site mutant protein. CTSL degrades MMP-2 at pH 5.5 and pH 7.0 (Fig. 6d), explaining higher protein amounts of MMP-2 upon Ctsl depletion. CTSB is able to degrade MMP-2 at pH 5.5 and pH 7.0 as well, but with lower efficiency than CTSL (Fig. 6e). This is reflected by a smaller increase of MMP-2 protein levels upon Ctsb depletion compared to Ctsl depletion. A strong accumulation of MMP-2 is observed upon Ctsb and Ctsl double deficiency (Fig. 5), highlighting a potential role of Ctsb and especially for Ctsl in MMP-2 degradation and processing. This represents a novel link between Ctsl and, to a lesser extent, Ctsb and MMP-2, creating a new bond in the protease web.

A degradative Ctsl—MMP-2 axis may affect extracellular protein abundance

In contrast to most altered proteins in the *Ctsb*$^{-/-}$ *Ctsl*$^{-/-}$ MEF secretome, MMP-2 protein levels increase (Table 2). Hence, we hypothesized that the decrease of some proteins in the secretome of *Ctsb*$^{-/-}$ *Ctsl*$^{-/-}$ MEFs may be due to increased degradation by elevated MMP-2 protein levels. To test this hypothesis, we added recombinant activated MMP-2 to the cell supernatant of wild-type MEFs and incubated the cells for 24 h. Afterwards, cell conditioned

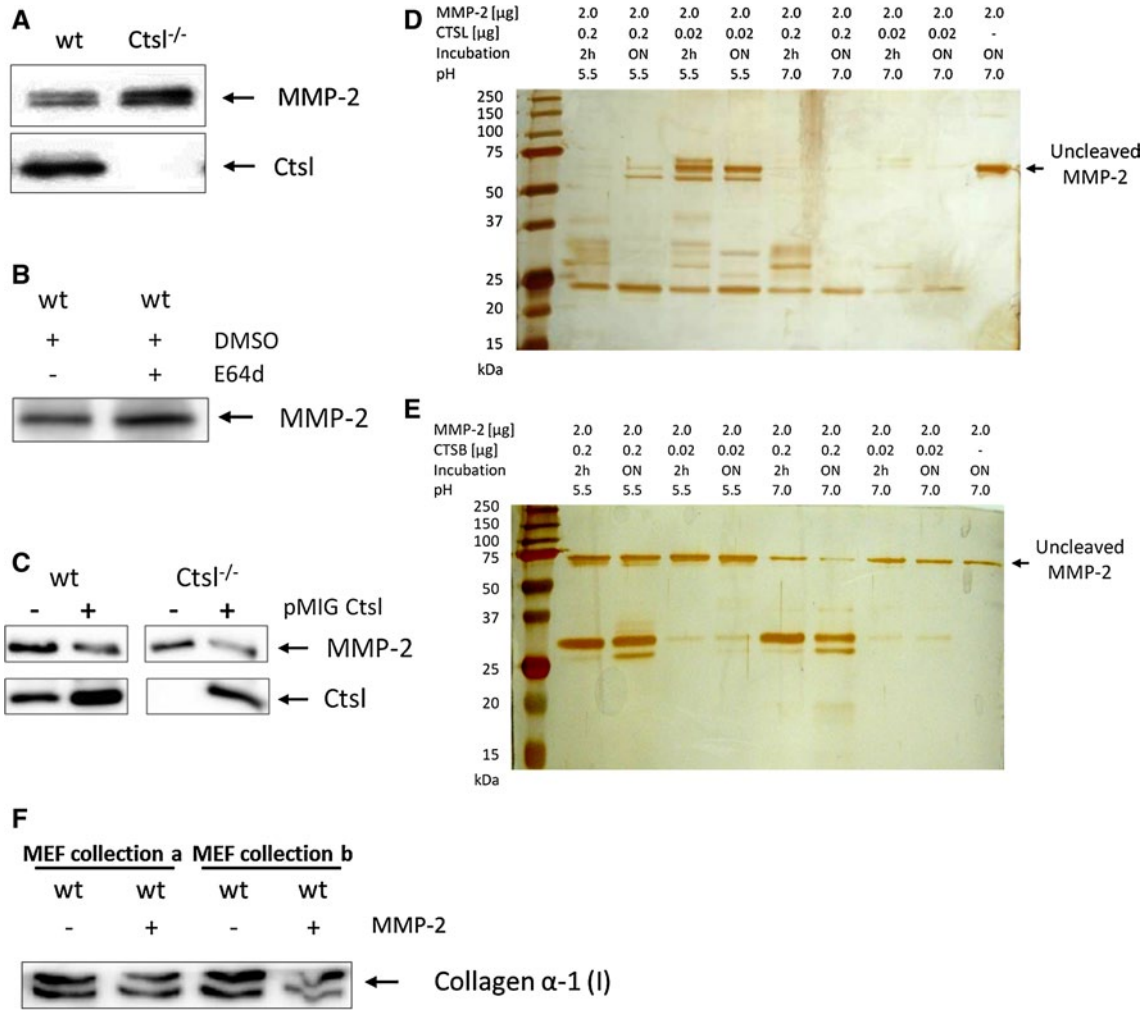

Fig. 6 **a** Western blot analysis of MMP-2 in cell-conditioned media of primary wild-type and Ctsl-deficient MEFs. **b** Western blot analysis of MMP-2 in cell-conditioned media of DMSO-treated wild-type MEFs and wild-type MEFs treated with 10 µM E64d for 48 h revealed an increase in MMP-2 protein levels upon cysteine cathepsin inhibition. DMSO served as solvent control. **c** Re-expression of Ctsl in Ctsl-deficient MEFs and overexpression in wild-type MEFs using the retroviral expression vector pMIG. Re-expression of Ctsl results in a decrease of MMP-2 protein levels. **d** CTSL cleaves human MMP-2 at 5.5 and 7.0. **e** CTSB cleaves human MMP-2 at 5.5 and 7.0, but with lower efficiency than CTSL. **f** Western blot analysis of cell-conditioned media of two wild-type MEF cell lines treated with activated pro-MMP-2 (125 ng/ml) compared to untreated cell-conditioned media. Pro-MMP-2 was activated by adding APMA for 3 h (details in "Materials and methods"). Collagen α-1 (I) protein levels decrease upon addition of activated pro-MMP-2 in both wild-type MEF cell lines. ON, overnight

media was concentrated and analyzed by Western blot. As MMP-2 is known as a collagen-degrading enzyme [71–73], addition of MMP-2 to the cell supernatant led to reduced collagen α-1 (I) protein levels (Fig. 6f).

These data indicate that Ctsl, and to a lesser extent Ctsb, are involved in MMP-2 degradation and processing, leading to a strong accumulation of MMP-2 in the secretome of *Ctsb*$^{-/-}$ *Ctsl*$^{-/-}$ MEFs. Higher protein levels of MMP-2 then result in a decrease of MMP-2 substrates such as collagen α-1 (I). This explanatory route fits to the overall profile of the secretome from Ctsb Ctsl double-deficient cells: while MMP–2 accumulates, almost all other significantly affected proteins display a decreased abundance.

Conclusion

This study presents a limited impact of Ctsb to secretome composition and extracellular proteolysis of MEFs. A more pronounced influence was observed for Ctsl in a previous study [13]. However, if both Ctsb and Ctsl are depleted, numerous proteins that remain unaffected upon single cathepsin deletion show strongly altered abundance. This highlights an impact of lysosomal proteases on secretome composition. Furthermore, it points to a cooperative function of Ctsb and Ctsl, especially in processes such as cell adhesion, ECM remodeling, signaling, and proteolytic regulation, and a collaboration of both proteases in vivo.

Loss of both Ctsb and Ctsl has a prominent effect on the abundance of numerous proteases and protease inhibitors, positioning Ctsb and Ctsl as key nodes in the "protease web." An important role for Ctsb and Ctsl in the proteolytic network was already described for skin proteolysis [14] and is highlighted in this study by a potential role of Ctsb and especially of Ctsl in MMP-2 degradation and processing. Whereas many proteins decrease, Western blot analysis corroborated increased MMP-2 protein levels in the Ctsb and Ctsl double-deficient secretome. Re-expression of Ctsl to the wild-type expression level resulted in decreasing MMP-2 protein levels, confirming the link between Ctsl and MMP-2. Since Ctsl does not affect gene expression, activation or secretion of MMP-2 [13], impaired MMP-2 degradation explains its increased protein levels. This is shown by in vitro cleavage assays, demonstrating that Ctsl and to a much lesser extent Ctsb are able to degrade MMP-2. Furthermore, addition of a cysteine protease inhibitor to the cell supernatant confirmed that accumulation of MMP-2 depends on cysteine cathepsin activity.

Higher protein levels of MMP-2 result in a decrease of MMP-2 substrates such as collagen α-1 (I). Since numerous other significantly affected proteins upon Ctsb and Ctsl double deficiency display a decreased abundance, a degradation of these proteins by MMP-2 can be hypothesized. These data support a strong impact of Ctsb and Ctsl on ECM composition via MMP-2 degradation.

Acknowledgments O.S. is supported by an Emmy-Noether grant from the Deutsche Forschungsgemeinschaft (DFG) (SCHI 871/2), a starting grant from the European Research Council (Programme "Ideas"—call identifier: ERC-2011-StG 282111-ProteaSys), and the Excellence Initiative of the German Federal and State Governments (EXC 294, BIOSS). J.N.K. acknowledges the Michael Smith Foundation for the Health Research (MSFHR) career investigator scholar award. T.R. is supported by Deutsche Forschungsgemeinschaft SFB 850 project B7 and grant Re158416-1, and furthermore by the Excellence Initiative of the German Federal and State Governments (EXC 294 and GSC-4, Spemann Graduate School). The authors thank Prof. Dr. Christoph Peters and Florian Christoph Sigloch for critical discussion. Franz Jehle and Bettina Mayer are acknowledged for excellent technical assistance. The authors thank Dr. Dorit Nägler, Munich, for the kind gift of recombinant CTSB and CTSL, Dr. Ulrich Maurer, Freiburg, for assistance with the pMIG system, and Dr. Gill Murphy for kindly providing recombinant human MMP-2. The core facility of the Universitätsklinikum Freiburg (Dr. Marie Follo and Klaus Geiger) is acknowledged for sorting cell lines.

Conflict of interest The authors declare no conflict of interest.

References

1. Turk V, Turk B, Turk D (2001) Lysosomal cysteine proteases: facts and opportunities. EMBO J 20(17):4629–4633. doi:10.1093/emboj/20.17.4629
2. Rawlings ND, Barrett AJ, Bateman A (2010) MEROPS: the peptidase database. Nucleic Acids Res 38(Database issue):D227–233. doi:10.1093/nar/gkp971
3. Aronson NN Jr, Barrett AJ (1978) The specificity of cathepsin B. Hydrolysis of glucagon at the C-terminus by a peptidyldipeptidase mechanism. Biochem J 171(3):759–765
4. Barbarin A, Frade R (2011) Procathepsin L secretion, which triggers tumor progression, is regulated by Rab4A in human melanoma cells. Biochem J. doi:10.1042/BJ20110361
5. Joyce JA, Baruch A, Chehade K, Meyer-Morse N, Giraudo E, Tsai FY, Greenbaum DC, Hager JH, Bogyo M, Hanahan D (2004) Cathepsin cysteine proteases are effectors of invasive growth and angiogenesis during multistage tumorigenesis. Cancer Cell 5(5):443–453
6. Jane DT, Morvay L, Dasilva L, Cavallo-Medved D, Sloane BF, Dufresne MJ (2006) Cathepsin B localizes to plasma membrane caveolae of differentiating myoblasts and is secreted in an active form at physiological pH. Biol Chem 387(2):223–234. doi:10.1515/BC.2006.030
7. Brix K, Dunkhorst A, Mayer K, Jordans S (2008) Cysteine cathepsins: cellular roadmap to different functions. Biochimie 90(2):194–207. doi:10.1016/j.biochi.2007.07.024
8. Mohamed MM, Sloane BF (2006) Cysteine cathepsins: multifunctional enzymes in cancer. Nat Rev Cancer 6(10):764–775. doi:10.1038/nrc1949
9. Reiser J, Adair B, Reinheckel T (2010) Specialized roles for cysteine cathepsins in health and disease. J Clin Invest 120(10):3421–3431. doi:10.1172/JCI42918
10. Gocheva V, Zeng W, Ke D, Klimstra D, Reinheckel T, Peters C, Hanahan D, Joyce JA (2006) Distinct roles for cysteine cathepsin genes in multistage tumorigenesis. Genes Dev 20(5):543–556. doi:10.1101/gad.1407406
11. Sevenich L, Werner F, Gajda M, Schurigt U, Sieber C, Muller S, Follo M, Peters C, Reinheckel T (2011) Transgenic expression of human cathepsin B promotes progression and metastasis of polyoma-middle-T-induced breast cancer in mice. Oncogene 30(1):54–64. doi:10.1038/onc.2010.387
12. Greenbaum D, Luscombe NM, Jansen R, Qian J, Gerstein M (2001) Interrelating different types of genomic data, from proteome to secretome: 'oming in on function. Genome Res 11(9):1463–1468. doi:10.1101/gr.207401
13. Tholen S, Biniossek ML, Gessler AL, Muller S, Weisser J, Kizhakkedathu JN, Reinheckel T, Schilling O (2011) Contribution of cathepsin L to secretome composition and cleavage pattern of mouse embryonic fibroblasts. Biol Chem 392(11):961–971. doi:10.1515/BC.2011.162
14. Tholen S, Biniossek ML, Gansz M, Gomez-Auli A, Werner F, Noel A, Kizhakkedathu JN, Boerries M, Busch H, Reinheckel T, Schilling O (2012) Deletion of cysteine cathepsins B or L yields differential impacts on murine skin proteome and degradome. Mol Cell Proteomics. doi:10.1074/mcp.M112.017962
15. Felbor U, Kessler B, Mothes W, Goebel HH, Ploegh HL, Bronson RT, Olsen BR (2002) Neuronal loss and brain atrophy in mice lacking cathepsins B and L. Proc Natl Acad Sci USA 99(12):7883–7888. doi:10.1073/pnas.112632299
16. Koike M, Shibata M, Waguri S, Yoshimura K, Tanida I, Kominami E, Gotow T, Peters C, von Figura K, Mizushima N, Saftig P, Uchiyama Y (2005) Participation of autophagy in storage of lysosomes in neurons from mouse models of neuronal ceroid-lipofuscinoses (Batten disease). Am J Pathol 167(6):1713–1728. doi:10.1016/S0002-9440(10)61253-9
17. Stahl S, Reinders Y, Asan E, Mothes W, Conzelmann E, Sickmann A, Felbor U (2007) Proteomic analysis of cathepsin B- and L-deficient mouse brain lysosomes. Biochim Biophys Acta 1774(10):1237–1246. doi:10.1016/j.bbapap.2007.07.004
18. Boersema PJ, Raijmakers R, Lemeer S, Mohammed S, Heck AJ (2009) Multiplex peptide stable isotope dimethyl labeling for quantitative proteomics. Nat Protoc 4(4):484–494. doi:10.1038/nprot.2009.21

19. Guo K, Ji C, Li L (2007) Stable-isotope dimethylation labeling combined with LC-ESI MS for quantification of amine-containing metabolites in biological samples. Anal Chem 79(22):8631–8638. doi:10.1021/ac0704356
20. Kleifeld O, Doucet A, auf dem Keller U, Prudova A, Schilling O, Kainthan RK, Starr AE, Foster LJ, Kizhakkedathu JN, Overall CM (2010) Isotopic labeling of terminal amines in complex samples identifies protein N-termini and protease cleavage products. Nat Biotechnol 28(3):281–288. doi:10.1038/nbt.1611
21. Molloy MP, Brzezinski EE, Hang J, McDowell MT, VanBogelen RA (2003) Overcoming technical variation and biological variation in quantitative proteomics. Proteomics 3(10):1912–1919. doi:10.1002/pmic.200300534
22. Dennemarker J, Lohmuller T, Muller S, Aguilar SV, Tobin DJ, Peters C, Reinheckel T (2010) Impaired turnover of autophagolysosomes in cathepsin L deficiency. Biol Chem 391(8):913–922. doi:10.1515/BC.2010.097
23. Morgenstern JP, Land H (1990) Advanced mammalian gene transfer: high titre retroviral vectors with multiple drug selection markers and a complementary helper-free packaging cell line. Nucleic Acids Res 18(12):3587–3596
24. Soneoka Y, Cannon PM, Ramsdale EE, Griffiths JC, Romano G, Kingsman SM, Kingsman AJ (1995) A transient three-plasmid expression system for the production of high titer retroviral vectors. Nucleic Acids Res 23(4):628–633
25. Pedrioli PG, Eng JK, Hubley R, Vogelzang M, Deutsch EW, Raught B, Pratt B, Nilsson E, Angeletti RH, Apweiler R, Cheung K, Costello CE, Hermjakob H, Huang S, Julian RK, Kapp E, McComb ME, Oliver SG, Omenn G, Paton NW, Simpson R, Smith R, Taylor CF, Zhu W, Aebersold R (2004) A common open representation of mass spectrometry data and its application to proteomics research. Nat Biotechnol 22(11):1459–1466. doi:10.1038/nbt1031
26. Kessner D, Chambers M, Burke R, Agus D, Mallick P (2008) ProteoWizard: open source software for rapid proteomics tools development. Bioinformatics 24(21):2534–2536. doi:10.1093/bioinformatics/btn323
27. Craig R, Beavis RC (2004) TANDEM: matching proteins with tandem mass spectra. Bioinformatics 20(9):1466–1467. doi:10.1093/bioinformatics/bth092
28. Keller A, Nesvizhskii AI, Kolker E, Aebersold R (2002) Empirical statistical model to estimate the accuracy of peptide identifications made by MS/MS and database search. Anal Chem 74(20):5383–5392
29. Cochrane GR (2010) The Universal Protein Resource (UniProt) in 2010. Nucleic Acids Res 38(Database issue):D142–148. doi:10.1093/nar/gkp846
30. Martens L, Vandekerckhove J, Gevaert K (2005) DBToolkit: processing protein databases for peptide-centric proteomics. Bioinformatics 21(17):3584–3585. doi:10.1093/bioinformatics/bti588
31. Li XJ, Zhang H, Ranish JA, Aebersold R (2003) Automated statistical analysis of protein abundance ratios from data generated by stable-isotope dilution and tandem mass spectrometry. Anal Chem 75(23):6648–6657. doi:10.1021/ac034633i
32. Mo F, Mo Q, Chen Y, Goodlett DR, Hood L, Omenn GS, Li S, Lin B (2010) WaveletQuant, an improved quantification software based on wavelet signal threshold de-noising for labeled quantitative proteomic analysis. BMC Bioinform 11:219. doi:10.1186/1471-2105-11-219
33. Han DK, Eng J, Zhou H, Aebersold R (2001) Quantitative profiling of differentiation-induced microsomal proteins using isotope-coded affinity tags and mass spectrometry. Nat Biotechnol 19(10):946–951. doi:10.1038/nbt1001-946
34. Kleifeld O, Doucet A, Prudova A, Auf dem Keller U, Gioia M, Kizhakkedathu J, Overall CM (2011) System-wide proteomic identification of protease cleavage products by terminal amine isotopic labeling of substrates. Nat Prot 6(10):1578–1611. doi:10.1038/nprot.2011.382
35. Rappsilber J, Ishihama Y, Mann M (2003) Stop and go extraction tips for matrix-assisted laser desorption/ionization, nanoelectrospray, and LC/MS sample pretreatment in proteomics. Anal Chem 75(3):663–670
36. Pan C, Kumar C, Bohl S, Klingmueller U, Mann M (2009) Comparative proteomic phenotyping of cell lines and primary cells to assess preservation of cell type-specific functions. Mol Cell Proteomics 8(3):443–450. doi:10.1074/mcp.M800258-MCP200
37. Olsen JV, Ong SE, Mann M (2004) Trypsin cleaves exclusively C-terminal to arginine and lysine residues. Mol Cell Proteomics 3(6):608–614. doi:10.1074/mcp.T400003-MCP200
38. Stypmann J, Glaser K, Roth W, Tobin DJ, Petermann I, Matthias R, Monnig G, Haverkamp W, Breithardt G, Schmahl W, Peters C, Reinheckel T (2002) Dilated cardiomyopathy in mice deficient for the lysosomal cysteine peptidase cathepsin L. Proc Natl Acad Sci USA 99(9):6234–6239. doi:10.1073/pnas.092637699
39. Petermann I, Mayer C, Stypmann J, Biniossek ML, Tobin DJ, Engelen MA, Dandekar T, Grune T, Schild L, Peters C, Reinheckel T (2006) Lysosomal, cytoskeletal, and metabolic alterations in cardiomyopathy of cathepsin L knockout mice. Faseb J 20(8):1266–1268. doi:10.1096/fj.05-5517fje
40. Friedrichs B, Tepel C, Reinheckel T, Deussing J, von Figura K, Herzog V, Peters C, Saftig P, Brix K (2003) Thyroid functions of mouse cathepsins B, K, and L. J Clin Invest 111(11):1733–1745. doi:10.1172/JCI15990
41. Tobin DJ, Foitzik K, Reinheckel T, Mecklenburg L, Botchkarev VA, Peters C, Paus R (2002) The lysosomal protease cathepsin L is an important regulator of keratinocyte and melanocyte differentiation during hair follicle morphogenesis and cycling. Am J Pathol 160(5):1807–1821. doi:10.1016/S0002-9440(10)61127-3
42. Dean RA, Overall CM (2007) Proteomics discovery of metalloproteinase substrates in the cellular context by iTRAQ labeling reveals a diverse MMP-2 substrate degradome. Mol Cell Proteomics 6(4):611–623. doi:10.1074/mcp.M600341-MCP200
43. Planque C, Kulasingam V, Smith CR, Reckamp K, Goodglick L, Diamandis EP (2009) Identification of five candidate lung cancer biomarkers by proteomics analysis of conditioned media of four lung cancer cell lines. Mol Cell Proteomics 8(12):2746–2758. doi:10.1074/mcp.M900134-MCP200
44. Xu BJ, Yan W, Jovanovic B, An AQ, Cheng N, Aakre ME, Yi Y, Eng J, Link AJ, Moses HL (2010) Quantitative analysis of the secretome of TGF-beta signaling-deficient mammary fibroblasts. Proteomics 10(13):2458–2470. doi:10.1002/pmic.200900701
45. Makawita S, Smith C, Batruch I, Zheng Y, Ruckert F, Grutzmann R, Pilarsky C, Gallinger S, Diamandis EP (2011) Integrated proteomic profiling of cell line conditioned media and pancreatic juice for the identification of pancreatic cancer biomarkers. Mol Cell Proteomics 10(10):M111.008599. doi:10.1074/mcp.M111.008599
46. auf dem Keller U, Schilling O (2010) Proteomic techniques and activity-based probes for the system-wide study of proteolysis. Biochimie 92(11):1705–1714. doi:10.1016/j.biochi.2010.04.027
47. Prudova A, auf dem Keller U, Butler GS, Overall CM (2010) Multiplex N-terminome analysis of MMP-2 and MMP-9 substrate degradomes by iTRAQ-TAILS quantitative proteomics. Mol Cell Proteomics 9(5):894–911. doi:10.1074/mcp.M000050-MCP201
48. Buck MR, Karustis DG, Day NA, Honn KV, Sloane BF (1992) Degradation of extracellular-matrix proteins by human cathepsin B from normal and tumour tissues. Biochem J 282(Pt 1):273–278
49. Creemers LB, Hoeben KA, Jansen DC, Buttle DJ, Beertsen W, Everts V (1998) Participation of intracellular cysteine proteinases, in particular cathepsin B, in degradation of collagen in periosteal tissue explants. Matrix Biol 16(9):575–584

50. Guinec N, Dalet-Fumeron V, Pagano M (1993) "In vitro" study of basement membrane degradation by the cysteine proteinases, cathepsins B, B-like and L. Digestion of collagen IV, laminin, fibronectin, and release of gelatinase activities from basement membrane fibronectin. Biol Chem Hoppe Seyler 374(12):1135–1146
51. Vasiljeva O, Korovin M, Gajda M, Brodoefel H, Bojic L, Kruger A, Schurigt U, Sevenich L, Turk B, Peters C, Reinheckel T (2008) Reduced tumour cell proliferation and delayed development of high-grade mammary carcinomas in cathepsin B-deficient mice. Oncogene 27(30):4191–4199. doi:10.1038/onc.2008.59
52. Schilling O, Overall CM (2008) Proteome-derived, database-searchable peptide libraries for identifying protease cleavage sites. Nat Biotechnol 26(6):685–694. doi:10.1038/nbt1408
53. Schilling O, auf dem Keller U, Overall CM (2011) Factor Xa subsite mapping by proteome-derived peptide libraries improved using WebPICS, a resource for proteomic identification of cleavage sites. Biol Chem 392(11):1031–1037. doi:10.1515/BC.2011.158
54. Schilling O, Huesgen PF, Barre O, Auf dem Keller U, Overall CM (2011) Characterization of the prime and non-prime active site specificities of proteases by proteome-derived peptide libraries and tandem mass spectrometry. Nat Protoc 6(1):111–120. doi:10.1038/nprot.2010.178
55. Biniossek ML, Nagler DK, Becker-Pauly C, Schilling O (2011) Proteomic identification of protease cleavage sites characterizes prime and non-prime specificity of cysteine cathepsins B, L, and S. J Proteome Res 10(12):5363–5373. doi:10.1021/pr200621z
56. Bernhardt A, Kuester D, Roessner A, Reinheckel T, Krueger S (2010) Cathepsin X-deficient gastric epithelial cells in co-culture with macrophages: characterization of cytokine response and migration capability after Helicobacter pylori infection. J Biol Chem 285(44):33691–33700. doi:10.1074/jbc.M110.146183
57. Sevenich L, Schurigt U, Sachse K, Gajda M, Werner F, Muller S, Vasiljeva O, Schwinde A, Klemm N, Deussing J, Peters C, Reinheckel T (2010) Synergistic antitumor effects of combined cathepsin B and cathepsin Z deficiencies on breast cancer progression and metastasis in mice. Proc Natl Acad Sci USA 107(6):2497–2502. doi:10.1073/pnas.0907240107
58. Wille A, Gerber A, Heimburg A, Reisenauer A, Peters C, Saftig P, Reinheckel T, Welte T, Buhling F (2004) Cathepsin L is involved in cathepsin D processing and regulation of apoptosis in A549 human lung epithelial cells. Biol Chem 385(7):665–670. doi:10.1515/BC.2004.082
59. Szklarczyk D, Franceschini A, Kuhn M, Simonovic M, Roth A, Minguez P, Doerks T, Stark M, Muller J, Bork P, Jensen LJ, von Mering C (2011) The STRING database in 2011: functional interaction networks of proteins, globally integrated and scored. Nucleic Acids Res 39(Database issue):D561–568. doi:10.1093/nar/gkq973
60. Valenta T, Hausmann G, Basler K (2012) The many faces and functions of beta-catenin. EMBO J 31(12):2714–2736. doi:10.1038/emboj.2012.150
61. Adams PD, Enders GH (2008) Wnt-signaling and senescence: a tug of war in early neoplasia? Cancer Biol Ther 7(11):1706–1711
62. Caldwell GM, Jones CE, Taniere P, Warrack R, Soon Y, Matthews GM, Morton DG (2006) The Wnt antagonist sFRP1 is downregulated in premalignant large bowel adenomas. Br J Cancer 94(6):922–927. doi:10.1038/sj.bjc.6602967
63. Lah TT, Buck MR, Honn KV, Crissman JD, Rao NC, Liotta LA, Sloane BF (1989) Degradation of laminin by human tumor cathepsin B. Clin Exp Metastasis 7(4):461–468
64. Novinec M, Grass RN, Stark WJ, Turk V, Baici A, Lenarcic B (2007) Interaction between human cathepsins K, L, and S and elastins: mechanism of elastinolysis and inhibition by macromolecular inhibitors. J Biol Chem 282(11):7893–7902. doi:10.1074/jbc.M610107200
65. Malanchi I, Santamaria-Martinez A, Susanto E, Peng H, Lehr HA, Delaloye JF, Huelsken J (2012) Interactions between cancer stem cells and their niche govern metastatic colonization. Nature 481(7379):85–89. doi:10.1038/nature10694
66. Snider P, Hinton RB, Moreno-Rodriguez RA, Wang J, Rogers R, Lindsley A, Li F, Ingram DA, Menick D, Field L, Firulli AB, Molkentin JD, Markwald R, Conway SJ (2008) Periostin is required for maturation and extracellular matrix stabilization of noncardiomyocyte lineages of the heart. Circ Res 102(7):752–760. doi:10.1161/CIRCRESAHA.107.159517
67. Norris RA, Damon B, Mironov V, Kasyanov V, Ramamurthi A, Moreno-Rodriguez R, Trusk T, Potts JD, Goodwin RL, Davis J, Hoffman S, Wen X, Sugi Y, Kern CB, Mjaatvedt CH, Turner DK, Oka T, Conway SJ, Molkentin JD, Forgacs G, Markwald RR (2007) Periostin regulates collagen fibrillogenesis and the biomechanical properties of connective tissues. J Cell Biochem 101(3):695–711. doi:10.1002/jcb.21224
68. Curran S, Murray GI (1999) Matrix metalloproteinases in tumour invasion and metastasis. J Pathol 189(3):300–308. doi:10.1002/(SICI)1096-9896(199911)189:3<300:AID-PATH456>3.0.CO;2-C
69. Egeblad M, Werb Z (2002) New functions for the matrix metalloproteinases in cancer progression. Nat Rev Cancer 2(3):161–174. doi:10.1038/nrc745
70. Loffek S, Schilling O, Franzke CW (2011) Series "matrix metalloproteinases in lung health and disease": biological role of matrix metalloproteinases: a critical balance. Eur Respir J 38(1):191–208. doi:10.1183/09031936.00146510
71. Aimes RT, Quigley JP (1995) Matrix metalloproteinase-2 is an interstitial collagenase. Inhibitor-free enzyme catalyzes the cleavage of collagen fibrils and soluble native type I collagen generating the specific 3/4- and 1/4-length fragments. J Biol Chem 270(11):5872–5876
72. Okada Y, Morodomi T, Enghild JJ, Suzuki K, Yasui A, Nakanishi I, Salvesen G, Nagase H (1990) Matrix metalloproteinase 2 from human rheumatoid synovial fibroblasts. Purification and activation of the precursor and enzymic properties. Eur J Biochem 194(3):721–730
73. Seltzer JL, Eisen AZ, Bauer EA, Morris NP, Glanville RW, Burgeson RE (1989) Cleavage of type VII collagen by interstitial collagenase and type IV collagenase (gelatinase) derived from human skin. J Biol Chem 264(7):3822–3826
74. Kersey PJ, Duarte J, Williams A, Karavidopoulou Y, Birney E, Apweiler R (2004) The International Protein Index: an integrated database for proteomics experiments. Proteomics 4(7):1985–1988. doi:10.1002/pmic.200300721